



2D RESONANCES IN ALPINE VALLEYS IDENTIFIED FROM AMBIENT VIBRATION WAVEFIELDS

Daniel ROTEN¹, Cécile CORNOU, Sibylle STEIMEN, Donat FÄH and Domenico GIARDINI

SUMMARY

Although numerical simulations have for long shown the importance of 2D resonances in site effect estimations of sediment-filled valleys, this phenomenon is usually not taken into account by current hazard assessment techniques. We present an approach to identify the resonance behaviour of a typical Alpine valley by analysis of measured and simulated ambient noise records. The resonance frequencies of the fundamental mode SV and the fundamental and first higher mode of SH are identified from measured data with the reference station method, verifying results of a previous study (Steimen [17]). Patterns of amplification, particle motion and phase behaviour obtained from observed and synthetic noise correlate well with properties expected for 2D resonance; the phase properties show that these patterns can not be caused by propagating surface waves. We conclude that the noise wavefield at low frequencies (0.25 to 0.50 Hz) is dominated by 2D resonance, and that microtremor records may be used for identification of resonance modes in sediment-filled valleys.

INTRODUCTION

It is well established that site-effects caused by unconsolidated deposits must be included in hazard assessments, and instrumental and numerical techniques are now widely used to estimate amplifications caused by 1D site effects. However, numerical simulations have for long demonstrated the importance of considering 2D or 3D geometries, since effects related to such structures can cause amplifications significantly higher than the corresponding 1D values (e.g. Bard [4]).

Sediment-filled Alpine valleys are common examples of such 2D-sites. Depending on the valley geometry, two different effects can be distinguished:

1. In rather shallow valleys, the wavefield is dominated by laterally propagating surface waves generated at the valley edges. This effect is often observed in both synthetic (e.g. Bard [1]) and measured data (e.g. Chávez-García [5], Field [8]). Lateral variations of the interface between bedrock and sediments can give rise to local resonances (Fäh [7]).
2. In deeper valleys, the interference of these surface waves with vertically propagating waves gives rise to the evolution of a 2D resonance pattern. Although this phenomenon evolved in many numerical simulations (e.g. Bard [4], Frischknecht [10]), observations on real data are rare (e.g. Tucker [11]).

Most attempts to identify and quantify these effects involved measurements of earthquake motion on different sites on the sediment fill and on the outcropping rock, using array-based (e.g. Cornou [3]) or reference station dependent (e.g. Chávez-García [5]) methods. In regions with low seismicity, site effect

¹Institute of Geophysics, ETH Zürich, Einstein Haus K29, Technoparkstr. 1, 8005 Zürich, Switzerland.
Email: daniel@seismo.ifg.ethz.ch

estimations using these procedures would require long and thereby expensive measurement campaigns. Methods based on quick and cheaper microtremor measurements for identification and quantification of such 2D-effects would therefore be desirable.

Steimen [17] analysed ambient vibration records acquired in the Rhône valley near Vétroz (Switzerland) with the site-to reference method and revealed some resonance properties of the sediment fill. Their results were further supported by numerical microtremor simulations computed with a realistic model of the Vétroz site. But since Steimen [17] used a single-station method, not measuring the ambient wavefield simultaneously across the valley, their observed data did not allow for a comparison of amplifications and phase characteristics of records acquired at different positions.

We present results of a new ambient vibration measurement campaign involving simultaneous recording at thirteen stations deployed across the valley and on the outcropping rock at the Vétroz site. The response of the site on microtremor will be further investigated using 3D numerical experiments acquired with state-of-the-art ambient vibration simulation methods.

We will seek for characteristic resonance patterns of the 2D-resonance wavefield by analysing spectral ratios, bandpass filtered traces and particle motion plots of measured and simulated records to investigate the following questions:

- Are the results of Steimen [17] confirmed by the use of simultaneous recordings?
- Can 2D resonance patterns be safely distinguished from laterally propagating surface waves? This problem is of special interest, since it gave rise to some discussion in recent publications (Paolucci [15], Chávez-García [6])
- Are microtremor records useful to assess site effect related to 2D structures?

GEOPHYSICAL MODEL

Based on results of a seismic reflection study done near Vétroz (Piffner [16]), Steimen [17] created a geophysical model of the site (Fig. 1 and Tab. 1). Shearwave velocities v_S were measured at the uppermost layer (Frischknecht [9]) and estimated for lower layers. Densities ρ are based on gravimetric studies, and quality factors Q_P and Q_S are estimated as well. The sediment thickness reaches 890 meters in the valley centre.

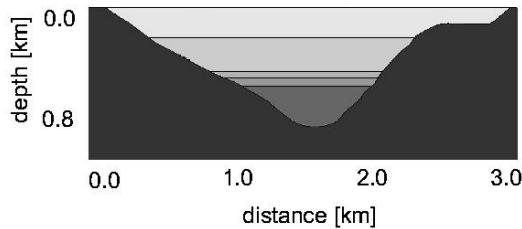


Figure 1: Cross section of Rhône valley at Vétroz site. See Table 1 for details of sediment fill. (modified from Steimen [17])

depth	v_P	v_S	Q_P	Q_S	ρ	geologic interpretation
0	1700	456	50	25	1900	deltaic sediments
210	1930	650	50	25	1900	glaciolacustrine deposits
470	1970	790	50	25	2000	meltout and reworked till
529	2300	920	50	25	2000	lodgment and till
584	2050	820	50	25	2000	subglacial deposit
890	5000	2890	200	100	2500	hard rock

Table 1: Geophysical model of the sediment fill. Depths are m, v_P and v_S in ms^{-1} and ρ in kgm^{-3}

PROPERTIES OF 2D RESONANCE MODES

Using the Aki-Lerner technique to simulate the seismic behaviour of a sine shaped valley on incident SH, SV and P-waves, Bard [4] showed the existence of three fundamental modes (Fig. 2).

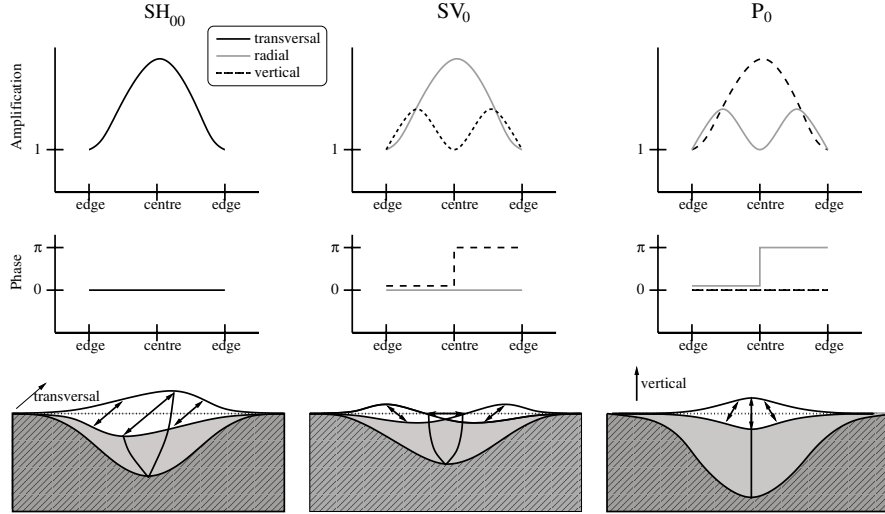


Figure 2: Amplification, phase and particle motion of the three fundamental modes of a sine shaped valley for the corresponding critical shape ratio (modified from Bard[4] and Steimen [17]).

Following the notation of Steimen [17], we define horizontal motion parallel to the valley axis as transversal and horizontal motion perpendicular to it as radial (referred to as anti-plane resp. in-plane by Bard [4]). Only the transversal component is excited in the SH-mode, while the SV- and P-modes excite both the radial and vertical component. In the SH-case fundamental mode, the phase is the same across the valley, and the amplification reaches its maximum in the valley centre. The SV fundamental mode is characterised by a maximum amplification in the centre of the valley for the radial component and a central node and two maxima for the vertical component. In this mode, the phase is the same across the valley for the radial component, while the phase of the vertical motion changes at the valley centre. The P fundamental mode behaves just vice-versa (Fig. 2).

Since two-dimensional resonance patterns involve both vertical and horizontal interferences, they can only appear in relatively deep valleys. To identify valleys whose seismic behaviour is characterised by two-dimensional resonance, Bard [4] introduced the concept of the *critical shape ratio*. For sine-shaped valleys, the shape ratio is defined as the ratio of the maximum sediment thickness h to the valley half-width l . For arbitrarily shaped valleys, this parameter is replaced by the 'equivalent' shape ratio $h/2w$, where $2w$ is defined as the total width over which the sediment thickness is more than half its maximum value. The critical shape ratio depends on the velocity contrast between bedrock and sediment fill (Fig. 3). If the shape ratio of a valley is above the critical value, its seismic behaviour at low frequencies will mainly be characterised by two-dimensional resonance. The critical shape ratio depends also on the wave type; its value is higher for P-waves than for SH- and SV-waves (Fig. 2).

Using 1750 m for $2w$ and 890 m for h (Fig. 1), we can assign a shape ratio of about 0.50 to the Rhône valley at the Vétroz site. In Figure 3, this shape ratio is indicated in the diagram for the velocity contrast obtained with the travelttime-based shearwave velocity average, showing that this site is clearly located in the domain of 2D resonance for the SH-case.

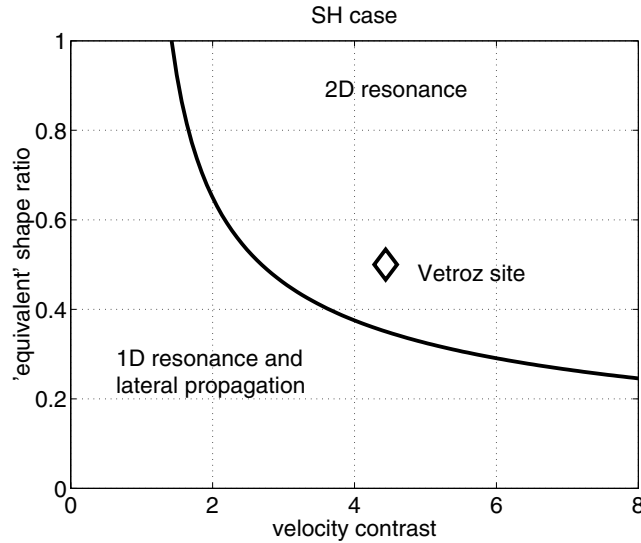


Figure 3: Critical shape ratio as a function of the velocity contrast for the SH case. The position of the Vétroz site was obtained with a shape ratio of 0.50 and the traveltime-based shearwave velocity average of Tab.1 (modified from Bard[4]).

METHOD

The experiments with real and simulated data were designed for a simultaneous examination of phase behaviour, amplification and particle motion at different points across the valley.

Field experiment

For the microtremor measurement we used 13 Lennartz three-component sensors with an eigenfrequency of 5 seconds. Data were recorded on Mars-88 loggers using DCF signals for time synchronisation; the sampling interval was 8 msec. Seven stations were deployed on a profile perpendicular to the axis of the valley, with shorter inter-station distances on the northern part (Fig. 4).

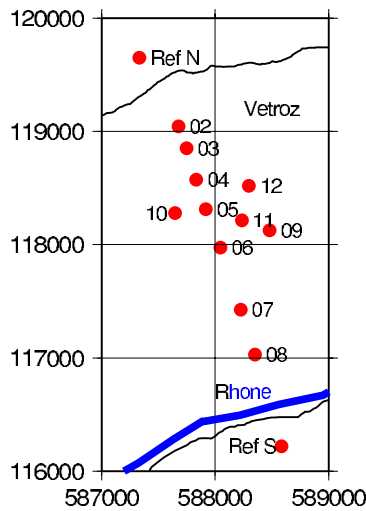


Figure 4: Configuration used for the microtremor measurement near Vétroz. Ticks denote the Swiss coordinate system in meters.

Four stations were set up outside the profile around the middle of the valley to form a small array; these stations are necessary to distinguish between laterally propagating surface waves and global resonance. The remaining two stations were used as reference stations on the North and on the South side of the profile on well-defined bedrock sites. The whole experiment took one day and yielded 90 minutes of simultaneous data on all stations.

Reference station method

The reference station approach is based on the assumption that the signal at the reference site represents the signal at the sediment-bedrock interface, which implies that source and path effects at both sites must be equal. The ratio of the Fourier spectra amplitude is used to estimate the transfer function between soil and rock site (e.g. Borchardt [2], Lermo [13]). When applied on earthquake data, the reference station method uses only the intense S-wave part of the seismograms. Applications on microtremors exploit the whole record regardless of the shape of the signals.

We used the same program as Steimen [17] for the calculation of reference spectra. This code splits time signals in 50% overlapping windows of 80 seconds using a trapezoidal taper. For each time window, the ratio of smoothed Fourier amplitudes is calculated and then averaged over all windows.

Numerical simulation of ambient vibrations

Steimen [17] modelled ambient vibrations with a source zone at the model boundary well away from the valley. This setup simulates the response of the structure to incoming waves similar to low-frequency microtremor mostly generated by sea surf.

To investigate the response of the site to ambient noise typical for densely-populated areas, we placed all sources randomly on the sediment surface inside the valley (Fig. 5). Each source is characterised by a random amplitude, direction and time function.

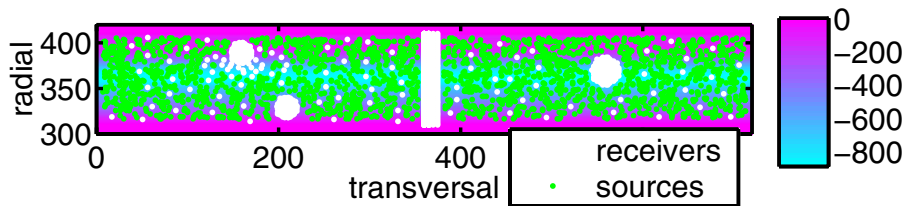


Figure 5: Source and receiver distribution and bedrock depth used for numerical simulation of ambient noise. Distances are in grid points. The box on the right is the colorbar of of the basin depth [m].

The wave propagation of this sources was calculated with an explicit heterogeneous finite-difference scheme developed within the SESAME project (Site Effects Assessments using Ambient excitations). The computational region is represented by a viscoelastic half-space with 3D surface heterogeneities and a planar surface (Moczo [14], Kristek [12]). The FD-grid is staggered and consists of a finer grid with 721x109x40 cells on the top and a coarser grid with 241x37x11 cells below; the spacing is 30 resp. 90 meters.

A number of receivers are distributed regularly along the valley surface; another set of receivers is placed to form four parallel lines running perpendicular to the profile axis. The remaining receivers are arranged in three dense arrays on the surface (Fig. 5).

EVIDENCE FOR 2D RESONANCE IN OBSERVED AMBIENT VIBRATIONS

Using the spectral ratio method, we first tried to determine the frequencies of possible resonance modes and then analysed the wavefield properties at the identified frequencies. Table 2 compares the values of the resonance frequencies of modes identified by Steimen [17] with our values.

	Steimen [17] modelled	Steimen [17] observed	this study modelled	this study observed
SV ₀	0.34±0.01	0.35±0.03	0.34±0.03	0.35±0.03
SH ₀₀	0.29±0.02	0.32±0.03	0.29±0.03	0.31±0.03
SH ₀₁	0.38±0.01		0.37±0.04	0.43±0.04
SH ₀₂	0.47±0.01		0.46±0.05	≈0.50

Table 2: Resonance frequencies [Hz] observed and measured by Steimen [17] and in this study.

Reference spectra from observations

Figure 6 shows average spectral ratios of all three components for all points on the profile axis (Points 2 to 8). One of the most distinct peaks can be found around 0.35 Hz on the radial component; this peak is also visible on the vertical axis, though the amplitude is much lower. On the radial component, the maximum amplitude at this frequency is reached on points 5 and 6 in the middle of the profile. This pattern is consistent with the fundamental mode SV wave, which was observed at 0.34 Hz by Steimen [17].

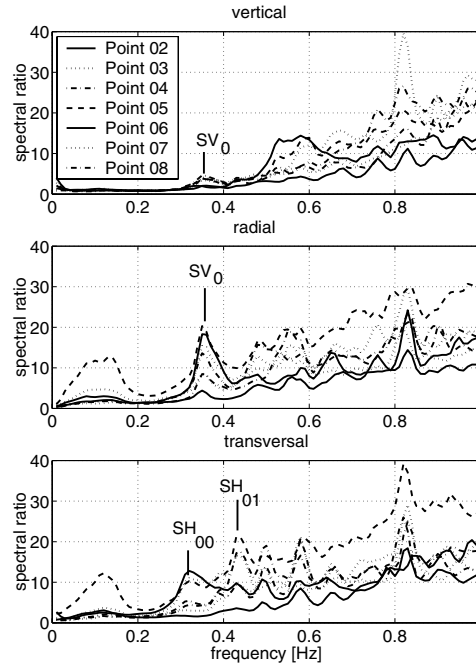


Figure 6: Average spectral ratios of points 2 to 8 calculated with the reference station in the North from about 60 minutes of noise.

On the transversal component, the first peak is located around 0.31 Hz, with high amplifications for points 5 to 7 in the valley centre. This is close to the value of 0.32 Hz assigned to SH₀₀ by Steimen [17]. Further peaks can be found around 0.43, 0.50 and 0.58 Hz; these peaks might correspond to higher modes of SH resonance.

Amplitude of spectral ratios related to identified resonance modes

In Figure 7, the mean spectral ratio and the standard deviation of the mean is shown as a function of distance along the profile for the radial and vertical component at 0.35 Hz.

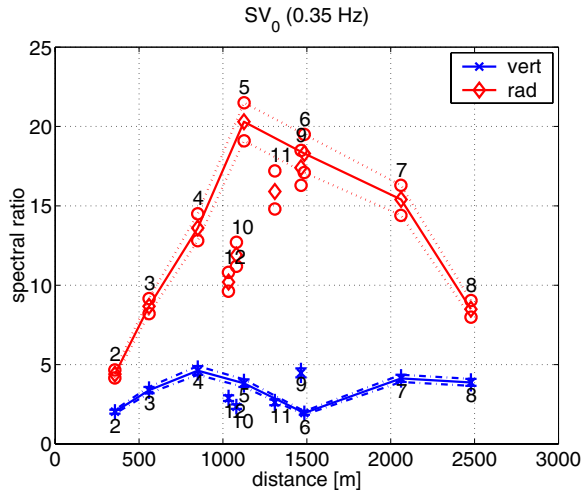


Figure 7: Average spectral ratios \pm one standard deviation of mean as a function of distance along the profile axis for the radial and vertical component at 0.35 Hz. Points lying on the profile axis are connected with lines. (Reference station North, about 60 minutes of noise)

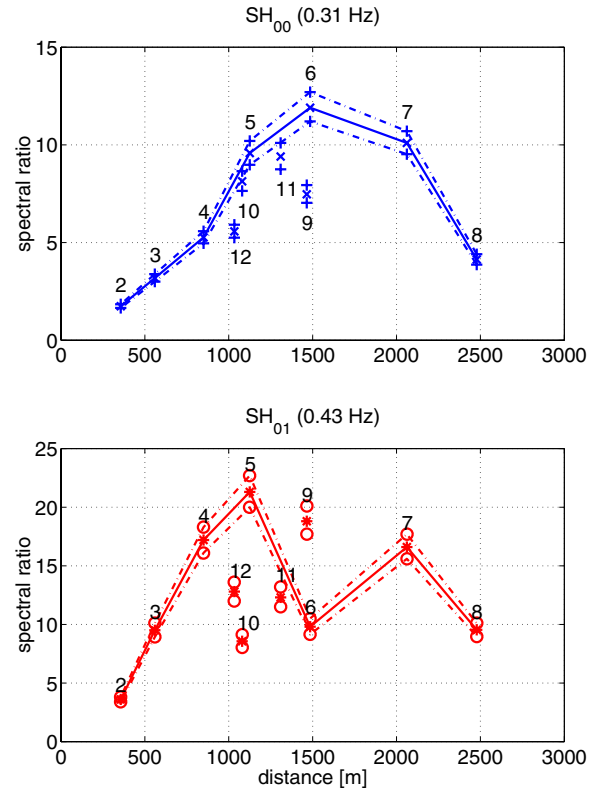


Figure 8: Average spectral ratios \pm one standard deviation of mean as a function of distance along the profile axis for transversal component at 0.31 Hz and 0.43 Hz. Points lying on the profile axis are connected with lines. (Reference station North, about 60 minutes of noise)

The pattern of spectral amplitude for points located on the profile axis is very close to the expected one (Fig. 2), with a maximum in the valley centre for the radial component and two maxima and one central node for the vertical component.

However, the spectral amplitude for points off the profile axis (point 9-12) clearly differs from points on the profile. The amplitude on the radial component at points 10 and 12 is lower than at points 4 and 5, although they are located at comparable distances from the valley border. The spectral amplitude of the vertical component at point 9 is significantly higher than at point 6, which exhibits a distinct node; but both points are located in the centre of the valley. Similarly, average spectral ratios of the transversal component at the resonance frequency of the fundamental SH mode (Fig. 8 top) compare well with the expected pattern (Fig. 2) for points located on the profile. But points located at distance from the line exhibit notably lower spectral amplitudes.

Figure 8 (bottom) shows the spectral ratio of the transversal component at 0.43 Hz, where we assumed the first higher SH mode from Figure 6. The spectral amplitude pattern for points on the profile is not too different from what we expect, showing two maxima and one central node, though the node is not very distinctive. Although possible higher modes of SH resonance were identified in Figure 6, the spatial sampling of the wavefield is too low to resolve the more complicated amplitude pattern at these frequencies.

Table 2 summarises the resonance frequencies identified in recorded microtremors. The uncertainties are based on the broadness of the peak and the variability of the amplification patterns with frequency.

Phase behaviour

In the fundamental mode SH resonance, the transversal motion is in phase at all points across the valley (Fig. 2). If the peak at 0.31 Hz in the spectral ratio is caused by the fundamental SH mode, this behaviour should also be visible on recorded bandpass filtered traces in this frequency range. Figure 9 (top) shows transversal components filtered between 0.28 and 0.34 Hz for all stations, demonstrating that both stations along the profile and stations outside the profile axis are nicely in phase.

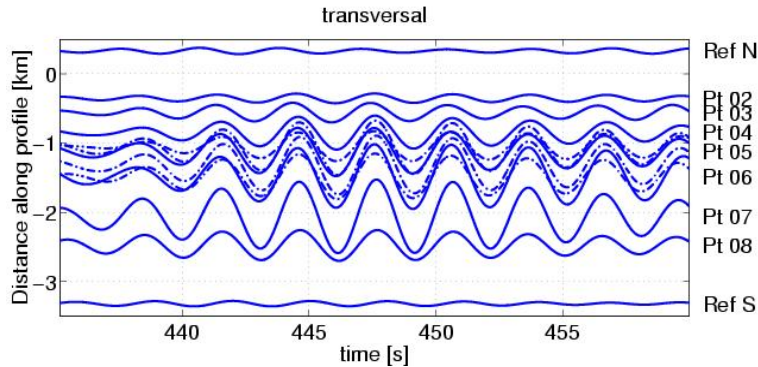


Figure 9: Time window of transversal components bandpass filtered around SH_{00} between 0.28 and 0.34 Hz. Seismograms of points outside the profile are printed with dashed lines.

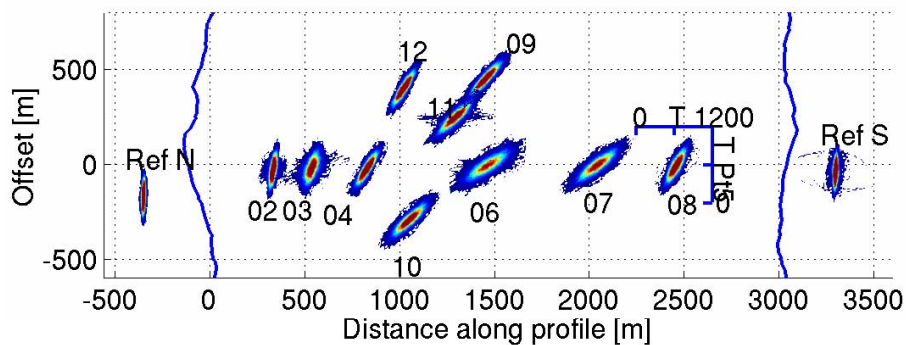


Figure 10: Phase behaviour of transversal components filtered between 0.28 and 0.34 Hz. See text for explanations.

The time window from Figure 9 also displays the increase of amplitude towards the valley centre.

To visualise the phase behaviour for longer time sections, the transversal motion for single station pairs is shown in Figure 10. Each plot is obtained by taking the transversal motion on point 5 in the valley centre on the vertical axis and the transversal motion of the actual point on the horizontal axis. If the signals are exactly in phase or antiphase, the curve should consist of a straight line running through the origin; the slope of the line is positive if signals are in phase and negative if they are in antiphase. A circular curve indicates out-of-phase behaviour. Colours display the number of times a point was sampled by the curve. While darkblue areas were touched just once, red areas were sampled multiple times, thus showing the predominant phase behaviour of the signals.

We can see from Figure 10 that these plots consist of ellipses for all points, and that the longer diameter of these ellipses shows a positive slope for all points within the valley. Areas of higher sampling resemble more narrow ellipses with similar orientation, suggesting that the motion is dominated by in-phase behaviour for the analysed record. The different slopes of the longer ellipse diameters reflect the amplitude of the transversal motion.

With the same methods, we can analyse the phase behaviour of the radial and vertical components at 0.35 Hz, where we identified the SV_0 resonance frequency with the reference station method. We would expect the radial component to be in phase on all points across the valley (Fig. 2), and the vertical component at points on the South side of the valley to be in antiphase with points on the North side. Figure

11 shows a time section of radial and vertical components filtered between 0.32 and 0.38 Hz. As expected, the radial component is in phase for both points along the profile as well as points outside the profile, showing a pattern similar to the transversal component at SH_{00} (Fig. 9).

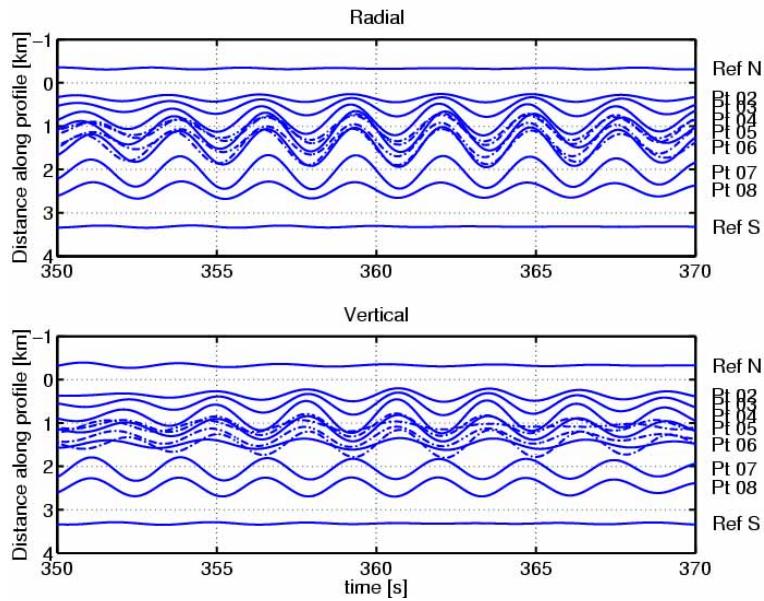


Figure 11: Time window of radial and vertical components filtered around SV_0 between 0.32 and 0.38 Hz. Seismograms of points outside the profile are printed with dashed lines.

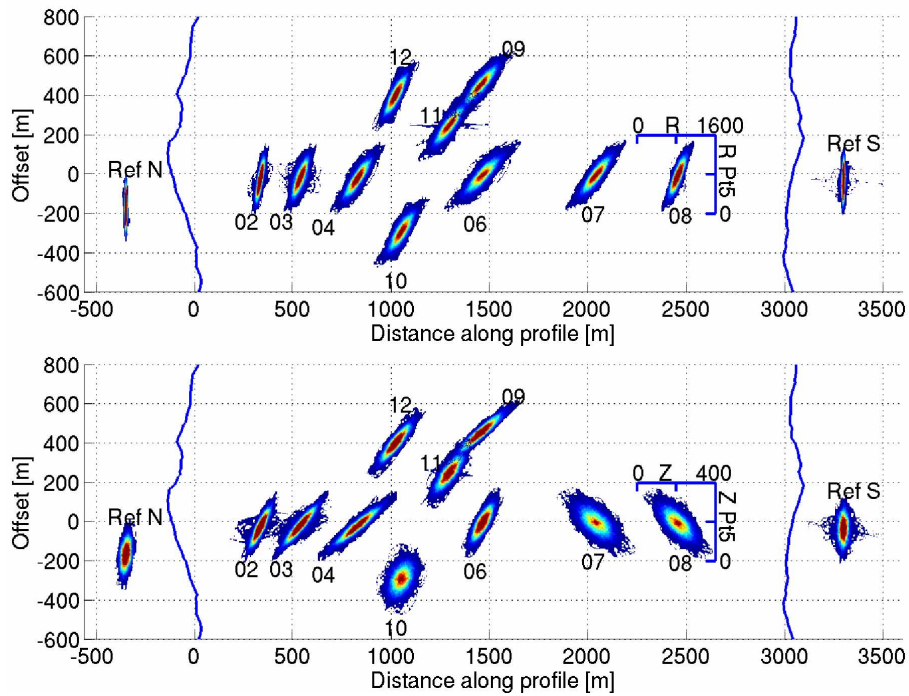


Figure 12: Phase behaviour of radial (top) and vertical (bottom) component filtered between 0.32 and 0.38 Hz. See text for explanations.

Motion on the vertical component, however, is only in phase for points on the Northern part. Traces on location 7 and 8 on the south are in antiphase with stations on the North side.

Again, we can display the phase behaviour for a larger time section by drawing components at individual points against a point in the centre (Fig. 12). For the radial component, the picture is similar to Figure 10, suggesting that signals at all points are in phase. On the vertical component, Points 7 and 8 are characterised by a less pronounced ellipse, with the longer diameter clearly exhibiting a negative slope. This confirms the pattern from Figure 11, which shows an anti-phase behaviour for these points.

Particle motion

The motion at the fundamental mode SV resonance is best visualised by a particle motion plot, which is obtained by drawing the radial against the vertical component at each station (Fig. 13). The motion is almost horizontal near the valley centre, where it reaches the highest amplitude. Towards the valley edges, the vertical component is increasing, resulting in an inclined movement aligned with the valley-bedrock interface (Fig. 2).

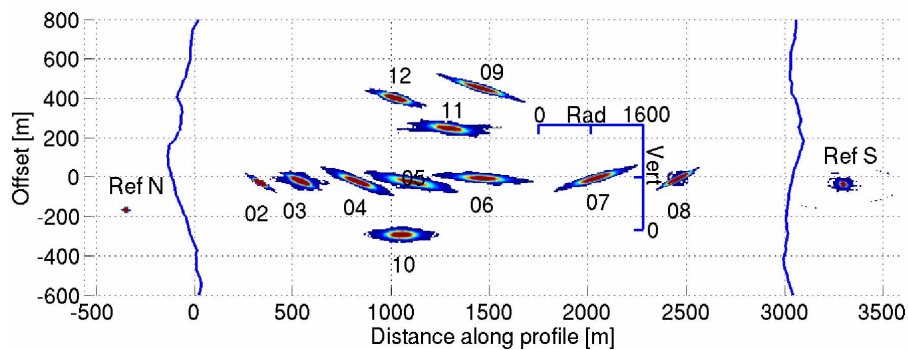


Figure 13: Particle motion plot of radial vs. vertical component obtained from traces bandpass filtered between 0.32 and 0.38 Hz.

PROPERTIES OF THE SYNTHETIC AMBIENT VIBRATION WAVEFIELD

We will now try to identify the 2D resonance modes we found in the measured data in synthetic seismograms, using the four parallel profiles in Figure 5. Since all sources are located on the sediment surface, the reference station method is not needed to study the valley response. Instead, the Fourier spectra at the different points can be examined directly. Averaging over windows was not applied due to the short length (90 seconds) of synthetic ambient vibration records.

Power spectra

Figure 14 gives power spectra of the signals from the receivers located on the line at grid position 370 (Fig. 5). The fundamental mode SV resonance was identified at 0.35 Hz, with two peaks visible on the vertical (left) and one broad peak on the radial component (centre). This is identical with the value of SV_0 found in the measured data. However, from Figure 14 this mode could also be picked at slightly higher frequency (around 0.37 Hz), where the spectra show a comparable pattern.

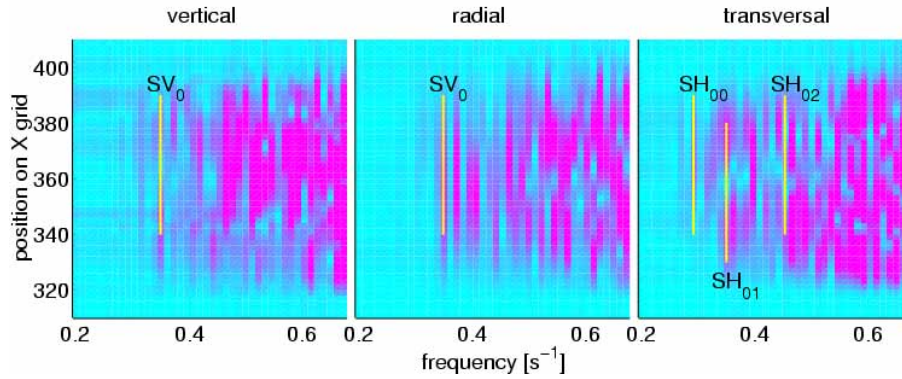


Figure 14: Power spectra of points located on profile at grid position 370. The amplitude is different for each component.

Similarly, values for the fundamental, first and second higher mode of SH are not unique (Fig. 14 bottom). They were identified at 0.29, 0.34 and 0.45 Hz (Fig. 14); these values are quite similar to those modelled by Steimen [17] with the same velocity model (Tab. 2)

Figure 15 (very left) shows a cross section of the radial and vertical Fourier amplitude at 0.35 Hz for all four profiles. The pattern corresponds to the SV fundamental mode predicted by theory (Fig. 2) and observed in real data (Fig. 7). The amplitude of the power spectrum varies for different cross-sections, especially on the radial component.

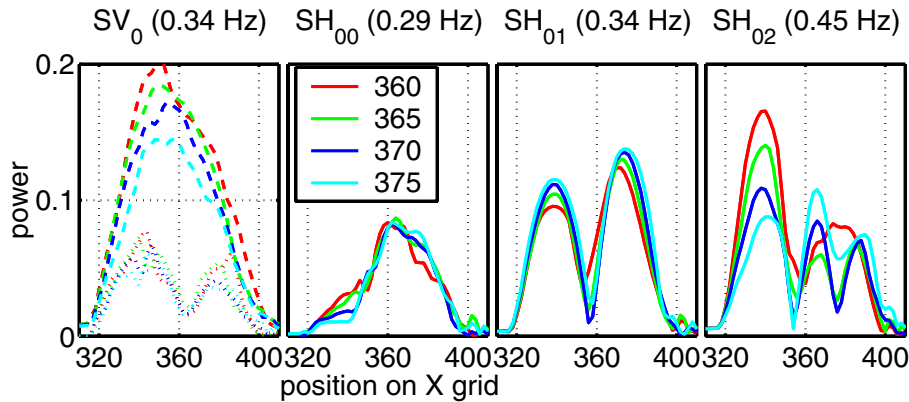


Figure 15: Cross sections of radial and vertical (dashed resp. dotted, left) and transversal (solid) power spectrum at different resonance frequencies for all four profiles.

Cross sections of the transversal component at the fundamental and first and second higher modes are displayed in Figure 15. At the fundamental mode frequency of 0.29 Hz, the cross-section exhibits an asymmetrical but well-defined single peak for all profiles. The first higher mode (0.34 Hz) is characterised by a central node and two maxima. For both modes, slight variations in the amplitude between the different profiles can be observed.

The cross section at 0.45 Hz (Fig. 15 right) shows two nodes and three peaks for three of the four profiles, similar to the pattern expected at the second higher mode. At this frequency, the four sections are quite different in shape and amplitude.

Phase behaviour

Finally, we will check if the phase behaviour predicted by theory and observed in real data can be identified in our ambient vibration simulations. Figure 16 shows a section of synthetic ambient noise records bandpass filtered at the corresponding SV and SH fundamental mode frequency.

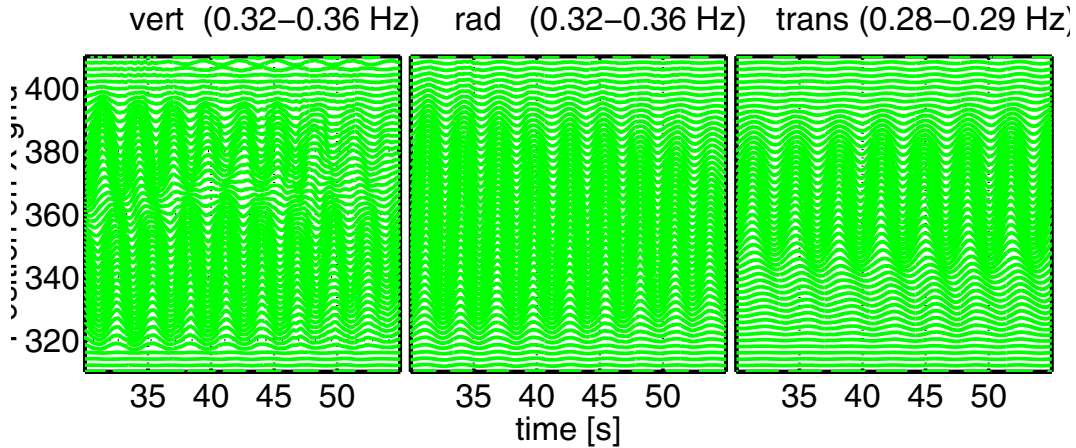


Figure 16: Bandpass filtered synthetic ambient noise records for all points on profile at grid position 370.

The bandpass was applied at the SV (vertical, radial) and SH (transversal) fundamental mode frequency. The vertical and radial components show a pattern similar to observed traces, with the radial components moving in phase and the vertical components in antiphase with receivers on the opposite valley side. The transversal components are also in phase on all stations across the valley. These observations are consistent with the behaviour predicted by theory (Fig. 2).

DISCUSSION

The spectral amplitude and phase patterns of SV_0 , SH_{00} and SH_{01} modes observed in recorded and simulated ambient noise correlate well with patterns predicted by theory, supporting the interpretation of these wavefield properties as a consequence of 2D resonance. These patterns can hardly be caused by laterally propagating surface waves, since the motion is in phase for both stations on as well as stations away from the profile. An interesting feature is the variability of the spectral amplitude with the position at equal distances from the valley border (Fig. 7 and 8). This may be explained as effect of the ambient vibration sources, because a certain variability was also observed in the synthetic ambient noise field (Fig. 15). Alternatively, these observations might be explained with the not perfectly two-dimensional structure of the valley.

The P-wave fundamental mode (P_0 in Fig. 2) was not identified in recorded or simulated data. This might be interpreted as a consequence of the physical and geometrical properties of the valley, since the P-mode requires a higher shape ratio (i.e. a deeper valley or lower velocities) than the SH- or SV-mode to develop.

The frequencies of SH_{01} and SH_{02} observed in recorded noise are notably higher than those identified in the simulation. This difference might be caused by discrepancies between real shearwave velocities and values used in the geophysical model (Tab. 1) or by the existence of non-planar layers in the sediment fill.

The uncertainties in the resonance frequencies identified in simulated data are higher than those reported by Steimen [17] (Tab. 2). This is probably a consequence of exciting the structure with ambient noise originating in the valley instead of laterally incident microtremor. However, our results show that 2D resonances can be excited by ambient noise characteristic for urban areas, which is relevant for the applicability of the method.

CONCLUSIONS

The resonance frequencies of the fundamental mode SV and the fundamental and first higher mode SH wave (Tab. 2) identified with the reference station method are in agreement with results published by Steimen [17].

Propagating surface waves can be precluded as explanation for the observed patterns in amplification and phase behaviour, leading to the conclusion that the noise wavefield is dominated by standing waves at low frequencies (0.25 to 0.50 Hz). But propagating waves do occur at higher frequencies, since they were identified in a small-scale array experiment that aimed to resolve shearwave velocities of the sediments at the Vétroz site (unpublished results).

Our observations suggest that ambient noise recordings may be used to investigate the resonance behaviour of sediment-filled valleys.

ACKNOWLEDGEMENTS

We thank Peter Moczo and Josef Kristek for using their FD code.

REFERENCES

1. Bard, P.-Y. and Bouchon, M. "The seismic response of sediment-filled valleys. Part 2. The case of incident P and SV waves". *Bull. Seism. Soc. Am.*, 1980; **70**(5), 1921-1941
2. Borchardt, R.D. "Effects of local geology on ground motion near San Francisco Bay." *Bull. Seism. Soc. Am.*, 1970; **60**, 29-61
3. Cornou, C., Bard, P.-Y. and Dietrich, M. "Contribution of Dense Array Analysis to the Identification and Quantification of Basin-Edge-Induced Waves, Part I; Methodology". *Bull. Seism. Soc. Am.*, 2003; **93**(6), 2604-2623
4. Bard, P.-Y. and Bouchon, M. "The two-dimensional resonance of sediment-filled valleys". *Bull. Seism. Soc. Am.*, 2000; **75**(2), 519-541
5. Chávez-García, F. J., Castillo, J. and Stephenson, W. R. "3D Site Effects; A Thorough Analysis of a High-Quality Dataset", *Bull. Seism. Soc. Am.*, 2003; **92**(5), 1941 - 1951
6. Chávez-García, F. J., and Stephenson, W.R. "Reply to 'Comment on '3D Site Effects: A thorough analysis of a high-quality dataset' by F. J. Chávez-García, J. Castillo, and W. R. Stephenson,' by R. Paolucci and E. Faccioli.", *Bull. Seism. Soc. Am.*, 2003; **93**(5), 2306-2316.
7. Fäh, D., Suhadolc, P. and G. F. Panza "Variability of seismic ground motion in complex media: the case of a sedimentary basin in the Friuli (Italy) area.", *Journal of Applied Geophysics*, **30**, 131-148
8. Field, E. H. "Spectral amplification in a sediment-filled valley exhibiting clear basin-edge-induced waves", *Bull. Seism. Soc. Am.*, 1996; **86**, 991-1005
9. Frischknecht, C. "Seismic Soil Amplification in Alpine Valleys. A Case Study: The Rhône Valley, Valais, Switzerland." Ph.D. thesis, Sections des Sciences de la terre, Université de Genève, 2000
10. Frischknecht, C., Wagner, J.-J. "Seismic Soil Effect in an Embanked Deep Alpine Valley; A Numerical Investigation of Two-Dimensional Resonance". *Bull. Seism. Soc. Am.*, 2004; **94**(1), 171 - 186
11. King, J.L. and Tucker, B.E. "Observed variations of earthquake motion over a sediment-filled valley", *Bull. Seism. Soc. Am.*, 1984; **74**, 137-152

12. Kristek, J. and Moczo, P. and Archuleta, R. J. "Efficient methods to simulate planar free surfaces in the 3D 4th-order staggered-grid finite-difference schemes", *Studia Geophys. Geod.*, 2002; **46**, 355-381
13. Lermo, J. and Chávez-García, F. J. "Are Microtremors Useful in Site Response Evaluation? ", *Bull. Seism. Soc. Am.*, 1994; **85**(5), 1350-1364
14. Moczo, P. and Kristek, J. and Bystrický, "Efficiency and optimisation of the 3D finite-difference modelling of seismic ground motion", *J. Comp. Acoustic*, 2001; **9**(2), 593-609
15. Paolucci, R., Faccioli, E., "Comment on '3D Site Effects: A thorough analysis of a high-quality dataset' by F. J. Chávez-García, J. Castillo, and W. R. Stephenson", *Bull. Seism. Soc. Am.*, 2003; **93**(5), 2301-2305
16. Pfiffner, O. A., Heitzmann, S., Mueller, S. and Steck, A. *Deep Structure of the Swiss Alps - Results of NRP 20*, 1997, Birkhäuser Basel, **21**, 265-276
17. Steimen, S., Fäh, D., Kind, F., Schmid, C., Giardini, D., "Identifying 2D Resonance in Microtremor Wave Fields", *Bull. Seism. Soc. Am.*, 2003; **93**(2), 583-599